Available online at www.sciencedirect.com
SCIENCE DIRECT®
ELSEVIER
Nuclear Instruments and Methods in Physics Research A 544 (2005) 565–576
NUCLEAR INSTRUMENTS & METHODS IN PHYSICS RESEARCH Section A
www.elsevier.com/locate/nima

EMMA: A recoil mass spectrometer for ISAC-II at TRIUMF

Barry Davids[a,*], Cary N. Davids[b]

[a]*TRIUMF, 4004 Wesbrook Mall, Vancouver BC, Canada V6T 2A3*
[b]*Physics Division, Argonne National Laboratory, Argonne IL 60439, USA*

Received 13 September 2004; received in revised form 5 January 2005; accepted 7 January 2005
Available online 11 March 2005

Abstract

Design work has begun on EMMA, an electromagnetic mass analyzer for ISAC-II at TRIUMF. EMMA is a recoil mass spectrometer that will be used to separate the recoils of nuclear reactions from the beam, and to disperse them according to mass/charge. ISAC-II will provide intense, low-emittance beams of unstable nuclei with masses up to 150 u and maximum energies of at least 6.5 MeV/nucleon. EMMA will be used in many different types of experiments with radioactive beams, especially those involving fusion-evaporation and transfer reactions. As such, it must be both efficient and selective, possessing large acceptances in angle, mass, and energy without sacrificing the necessary beam suppression and mass resolution.

PACS: 07.75.th; 25.60.−t; 29.30.Aj

Keywords: Recoil mass spectrometer; Electromagnetic separator; Recoil separator

1. Introduction

An electromagnetic mass analyzer, EMMA, is planned for use with the heavy radioactive ion beams that will be available from the ISAC-II facility at TRIUMF. ISAC-II will provide intense, high-quality beams of radioactive ions with masses up to 150 u and maximum energies of at least 6.5 MeV/nucleon [1]. These beams will allow the study of the single-particle structure of exotic nuclei, the evolution of nuclear structure and shapes far from stability and at high spin, fundamental symmetries, and nuclear astrophysics. Some of the techniques needed to explore these subjects include Coulomb excitation, fusion evaporation, and transfer reactions initiated by heavy radioactive ions in inverse kinematics. The study of many of these reactions will require detection and identification of the heavy recoil nucleus, in addition to light charged particles, neutrons, and γ rays. The former will be the purpose of EMMA, a recoil mass spectrometer designed to separate the recoils of a nuclear

*Corresponding author.
E-mail address: davids@triumf.ca (B. Davids).

0168-9002/$ - see front matter © 2005 Elsevier B.V. All rights reserved.
doi:10.1016/j.nima.2005.01.297

reaction from the primary beam, and to disperse them in a focal plane according to their mass-to-charge ratio (M/q).

In the recent past, several different types of ion-optical configurations have been employed to fulfill roles similar to that envisioned for EMMA at ISAC-II. The first is a velocity filter that uses a Wien filter or separated electric dipole (ED) and magnetic dipole (MD) fields to disperse beam and recoils according to velocity. An example of this type of recoil separator is SHIP at GSI [2]. A second type is a gas-filled recoil separator, which relies on collisions of heavy ions with a dilute gas filling a magnetic spectrometer to separate beam and recoils. RITU in Jyväskylä [3] is such a separator. Thirdly, there are large acceptance magnetic spectrometers such as PRISMA at INFN Legnaro [4] and MAGNEX at LNS Catania [5]. In addition, there is the hybrid spectrometer VAMOS at GANIL [6], which incorporates a Wien filter in a magnetic spectrometer. Finally there are vacuum-mode recoil mass spectrometers based on EDs and MDs which disperse according to M/q instead of velocity. The first such device was built at the University of Rochester [7,8], and several similar spectrometers have been constructed around the world. A recent review of gas-filled separators can be found in Ref. [9], and vacuum-mode separators are reviewed briefly in Ref. [10].

2. Scientific program

EMMA will be an integral part of the experimental program at ISAC-II, both as a stand-alone device and in conjunction with other detection systems. One important avenue of research will involve the coupling of EMMA with the advanced γ ray detector array TIGRESS [11]. By positioning TIGRESS around the target position of EMMA, prompt γ rays emitted by a recoiling nucleus formed in a fusion-evaporation or transfer reaction can be correlated with the arrival of the recoil at the focal plane of EMMA. Focal plane detectors will allow the determination of the mass and in many cases the atomic number of the recoil using position, energy loss, and time-of-flight measurements. The recoil information allows very weak reaction channels to be studied in the presence of very high yield background channels, enabling the exploration of high spin states in exotic nuclei as well as their low-lying, single-particle structures.

By implanting the recoils in a double-sided silicon strip detector (DSSD), the full power of the recoil decay tagging technique can be employed. In this method, the observation of prompt γ rays near the target is combined with the detection of charged particles such as α particles, protons, and β-delayed protons emitted in the radioactive decay of mass-identified recoils implanted in a silicon detector behind the focal plane. Since typical flight times through EMMA will be $\lesssim 1\,\mu s$, short half-life radioactivities can be studied. Placing γ detectors at the focal plane will allow the study of μs isomers. Replacing the DSSD with a thin catcher foil and positioning silicon PIN diode detectors behind it will permit the detection of conversion electrons emitted in the decay of implanted recoils.

In transfer reactions, the detection of the light ejectile is essential for the measurement of the recoil excitation energy. For this purpose, a silicon strip detector array (e.g., Ref. [12]) would be positioned around the target position and operated in coincidence with the focal plane detectors of EMMA. These reactions can be used to measure the excitation energies, spins, and parities of low-lying levels in the recoil nucleus. Such studies are essential for elucidating the changes in nuclear structure away from stability, and for the determination of the properties of resonances important in nuclear astrophysics.

3. Implications of scientific aims for spectrometer design

Two types of reactions will place the most stringent demands on EMMA, fusion-evaporation and single-nucleon transfer in inverse kinematics. Though they are centred about 0°, the products of fusion-evaporation reactions emerge from the target with a relatively large spread in angle and energy. This spread depends on the reaction kinematics, including the ratio of beam and target

masses, the compound nucleus excitation energy, and the number of neutrons, protons, and α particles evaporated. Typical values are solid angles of 10–15 msr and $\pm$10–20% energy spreads [13]. Many interesting fusion-evaporation reaction channels have small cross-sections, so beam suppression must be high. For single-nucleon transfer reactions in inverse kinematics, the angular and energy spreads of the heavy recoils are very small, with typical laboratory frame recoil scattering angles less than 1° and energy spreads $\leqslant \pm 5\%$. Cross-sections are typically much larger than for rare fusion-evaporation channels, so beam suppression is not as critical, but it is a different challenge because both the momentum and the mass of the recoil are very close to those of the primary beam. Hence physical separation of adjacent masses as well as relatively high mass resolution are crucial. As beams of 150 u must be separated from far less abundant recoils differing by a single mass unit, a mass resolving power ($M/\Delta M$) greater than 400 FWHM will be required, as will be shown in Section 5. In addition, for heavy beams at Coulomb barrier energies, transfer reaction recoils are not fully stripped, and are therefore difficult to deflect due to their large electric rigidities.

We consider now the characteristics of the types of recoil separators described in the introduction with an eye toward the envisioned scientific programme of EMMA. Velocity filters have high transmission of recoils and excellent beam suppression for fusion-evaporation reactions. However, they have no mass resolving power since they disperse according to velocity rather than mass. Therefore in transfer reactions with heavy beams, in which the velocities of beam and recoil overlap due to finite beam energy spread, beam rejection is impossible, even if mass resolution were deemed dispensable. The same beam rejection problem exists for gas-filled recoil separators, which also efficiently transmit fusion-evaporation recoils, particularly in direct kinematics. The best mass resolving power that has been obtained [9], $\sim$50, is totally inadequate for transfer reaction work.

Recently, several laboratories have constructed large-acceptance magnetic spectrometers. These devices have angular acceptances $\geqslant$50 msr. Such large angles produce huge geometric aberrations that can only be partially corrected with hardware. Therefore ray tracing is required to reconstruct the momenta of the detected particles, since the image in the focal plane is distorted by the aberrations. Ray tracing is very problematic for low-energy heavy ions, since the interactions with even very thin position-sensitive detectors induce multiple scattering that changes the angles to be measured. Moreover, even if ray tracing were feasible, only the momentum/charge (p/q) of a particle would be measured. Such a measurement is of limited use for spectroscopy of a recoil nucleus with beams of mass 30 u or higher [14], because the resolution is too poor to yield useful information on the excitation energy of the recoil. In order to deduce the mass of a recoil, one needs to measure its time of flight as well. In practice, mass resolving power of 280 has been obtained in this way [4]. Magnetic spectrometers disperse according to p/q, so recoils and beam particles that have identical momenta and charge states will not be spatially separated at the focal plane (or anywhere else), in which case beam rejection at 0° is impossible. In practice, this means that magnetic spectrometers are not well suited to the study of single-nucleon transfer reactions with heavy beams, where finite beam energy spread implies an overlap between the magnetic rigidities of beam and recoil.

A hybrid device, such as a magnetic spectrometer that can be filled with gas and operated as a gas-filled recoil separator would be unsuitable for transfer reactions for the reasons outlined above. Similarly, adding a velocity filter to a magnetic spectrometer, as in VAMOS [6], does not seem to be a good compromise to meet the needs of ISAC-II users. The mass resolving power that can be obtained by operating VAMOS in this way is limited to 125 [15], which is much too low for single-nucleon transfer reactions with heavy beams.

EMMA will be used to separate recoils from the beam and to identify the recoils according to M/q. Measurements of the energy or momentum of recoils are in general insufficiently precise for spectroscopic purposes, so a magnetic spectrometer is the wrong tool. As will be shown in Section 5, the relative difference between the

central momenta of a recoil and a beam particle is similar in magnitude to their relative mass difference in a single-nucleon transfer reaction, but finite beam emittance implies that there will be overlap in the momentum distributions. In contrast, M/q is quantized, so there is no overlap between the M/q distributions of recoil and beam. Of course, finite M/q resolution will imply some degree of overlap between the spatial distributions in the focal plane of any real spectrometer, but a mass spectrometer optimally separates recoil and beam because it disperses according to a quantity that differs sharply between the two. In addition, one would like to have zero energy dispersion and angular focussing, so that all nuclei of a given M/q end up at the same position in the focal plane. This facilitates beam rejection for small mass differences, optimizes transmission efficiency, and allows implantation of mass-identified recoils into a compact detector for subsequent decay studies.

We conclude that the best design for EMMA will be an energy and angle focussing recoil mass spectrometer. Quite a few spectrometers of this kind have already been built and operated, including CAMEL at Legnaro [16–18], the FMA at Argonne [19–21], the Oak Ridge RMS [22–24], HIRA at NSC New Delhi [25], the JAERI RMS [26–28], and DRAGON at TRIUMF [29]. All but the last of these spectrometers are based on an EME design in which the energy dispersion created by the EDs (E) is cancelled by the momentum dispersion of the MD (M), resulting in mass dispersion. This scheme is superior to designs with only two bending elements such as CARP at RCNP Osaka [30], which have lower beam rejection and provide energy dispersion cancellation at only a single, fixed focal plane position. Spectrometers that make use of EDs have larger energy and M/q acceptances than those that rely on Wien filters such as the Daresbury recoil separator [31], ARES [32], and ERNA [33]. Therefore, we have opted for an EME design, and have worked toward increasing the energy and angular acceptances beyond what has been achieved in existing designs. At the same time, we have tried to avoid sacrificing M/q acceptance, beam rejection, bending power, and mass resolution.

4. Ion optics

The ion optics code GIOS [34] was used to lay out the configuration of magnetic and electric elements, calculate their properties, and optimize the design. In this code, the motion of a charged particle through electromagnetic fields is described relative to a reference trajectory, the optic axis, which is straight in quadrupole (Q) and multipole lenses, but curved in ED and MD bending elements. This reference trajectory is defined by the kinetic energy per charge E_0/q_0 and mass per charge M_0/q_0 of the reference particle. Trajectories are further defined by the initial position of the particle relative to the optic axis in the dispersive and non-dispersive directions, x and y. One must also specify the initial values of the variables a and b, which are defined by $a = p_x/p_0$ and $b = p_y/p_0$, where p_0 is the magnitude of the momentum of the reference particle, and p_x and p_y the projections of the particle momentum on the horizontal and vertical axes, respectively. Particles with different masses, energies, and charges are then included by specifying their fractional deviations from the mass per charge and kinetic energy per charge of the reference particle, δ_M and δ_E. If x, y, a, b, δ_M, and δ_E are small, it is possible to write the value of a quantity at any point in the device as a Taylor series expansion in terms of the initial values of these 6 variables. This type of expansion for paraxial rays is described in Ref. [35]. All of our calculations were performed to third order in the horizontal, dispersive direction, and second order in the vertical, nondispersive direction, which is adequate for the small initial values of the variables relevant to this design. Fringing fields for the electric and magnetic elements were included using the integral representation employed by GIOS. The values of these integrals were taken from the measured fringing fields of similar electric and magnetic elements.

The basic EME configuration is augmented with quadrupole lenses to increase the solid angle, allow variable mass dispersion, and improve the final vertical focus. Quadrupole doublets were found to give the best performance, and a symmetric configuration QQEMEQQ adopted. Fig. 1 schematically depicts EMMA as seen from above and

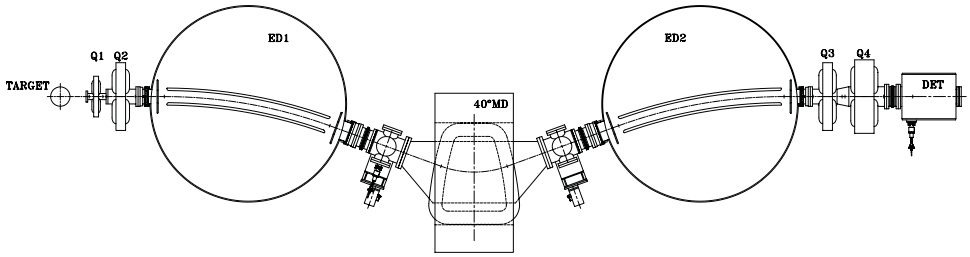

Fig. 1. Schematic view of EMMA, showing the target, quadrupole and dipole magnets, and EDs. The detector box is also indicated.

Table 1
EMMA dimensions and maximum fields

Length from target to focal plane (m)	9.04		
Dipoles	MD	ED1,ED2	
Radius of curvature (m)	1.0	5.0	
Deflection angle (°)	40	20	
Effective field boundary inclination angles (°)	8.3	0	
Effective field boundary radii (m)	3.472	—	
Gap (cm)	12	12.5	
Maximum field	1.0 T	50 kV/cm	
Maximum rigidity	1.0 T m	25 MV	
Magnetic lenses	Q1	Q2,Q3	Q4
Bore diameter (cm)	7	15	20
Effective length (cm)	14	30	40
Maximum pole tip field (T)	1.21	0.87	0.81
Maximum field gradient (T/m)	35	12	8.1

Table 1 lists its dimensions. The distance between the target and first quadrupole will be variable; the minimum separation required to accommodate the γ array TIGRESS is 30 cm. We note that the required maximum electric and magnetic field strengths have all been achieved with modern designs.

Care was taken to maximize angular, mass, and energy acceptance while minimizing geometric and chromatic aberrations. Magnetic multipoles for higher order correction were found to be unnecessary, a distinct advantage in terms of cost and ease of tuning. A single higher order correction was made by incorporating a curved effective field boundary into the MD. This correction was optimized by simultaneously minimizing the aberrations due to the $(x|\delta_E^2)$, $(x|a\delta_E)$, and $(x|a^2)$ terms.

In all of the calculations presented here, an M/q dispersion of 10 mm/% was chosen at an angular and energy focus 30 cm from the exit of the final quadrupole, and a uniform beam spot on the target of 1 mm × 1 mm was assumed. A separation between the target and first quadrupole of 30 cm was used. The mass focus is shown in Fig. 2, while Fig. 3 shows the energy focus, and Fig. 4 the spatial focus. A calculated mass spectrum centred about mass 100 is shown in Fig. 5.

Table 2 lists some of the calculated capabilities of EMMA. It is useful to compare these properties with the same values calculated for the FMA recoil mass spectrometer at Argonne National Laboratory [20]. Compared with the FMA, EMMA has a 25% larger maximum electric rigidity, a 14% larger mass acceptance, an equivalent energy acceptance, and a 100% larger solid angle with a more symmetric angular acceptance. In addition, the size of the dominant $(x|a^2)$ aberration is 30% smaller in EMMA than the FMA, resulting in higher mass resolution even with a larger solid angle.

5. Predicted performance for d(^{132}Sn,p)^{133}Sn

We now examine a specific reaction in order to illustrate how EMMA will be used in a prototypical experiment. As indicated in Section 3, the

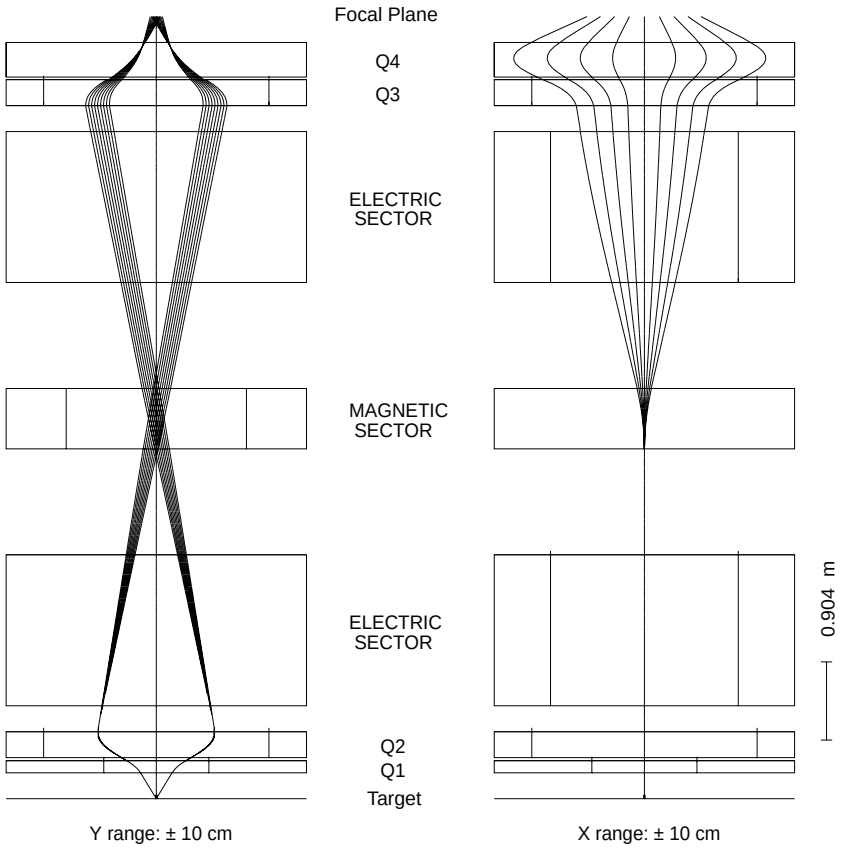

Fig. 2. Calculated mass focus of EMMA, showing rays corresponding to 9 adjacent masses emitted from the target with vertical angles of -2°, 0°, and 2°. At the focal plane, the 9 masses are seen to be dispersed horizontally and focussed vertically. Angular focussing in the horizontal direction is shown in Fig. 4.

separation from the beam and detection of the recoils from fusion-evaporation and transfer reactions are likely to be the principal uses of this device, and also place the most severe demands on its resolution, beam suppression, and acceptance. As the layout, design, and properties of EMMA are very similar to those of the FMA at Argonne National Laboratory [20], which has been operated successfully to study fusion-evaporation recoils for over a decade, we expect that EMMA will perform similarly to the FMA in this domain. Therefore, we concentrate here on a novel challenge, the separation of recoils differing by a single mass unit from a heavy beam in a transfer reaction at or above the Coulomb barrier. The example we choose is the reaction $d(^{132}Sn,p)^{133}Sn$ at a beam energy of 6 MeV/nucleon. At this energy, the angular distributions of the proton ejectiles differ sufficiently for different values of the transferred angular momentum to permit determination of the valence nucleon's orbital. These protons will be detected with a silicon strip detector array at the target in coincidence with recoils at the focal plane of EMMA. This reaction represents a demanding test for the spectrometer, in that the recoils are very rigid and therefore difficult to bend. Furthermore, the relative M/q difference between the recoils and the much more intense beam is less than 1%, so spatial separation and suppression of the beam are also nontrivial. The kinematics of the reaction are such that the interesting recoils corresponding to protons

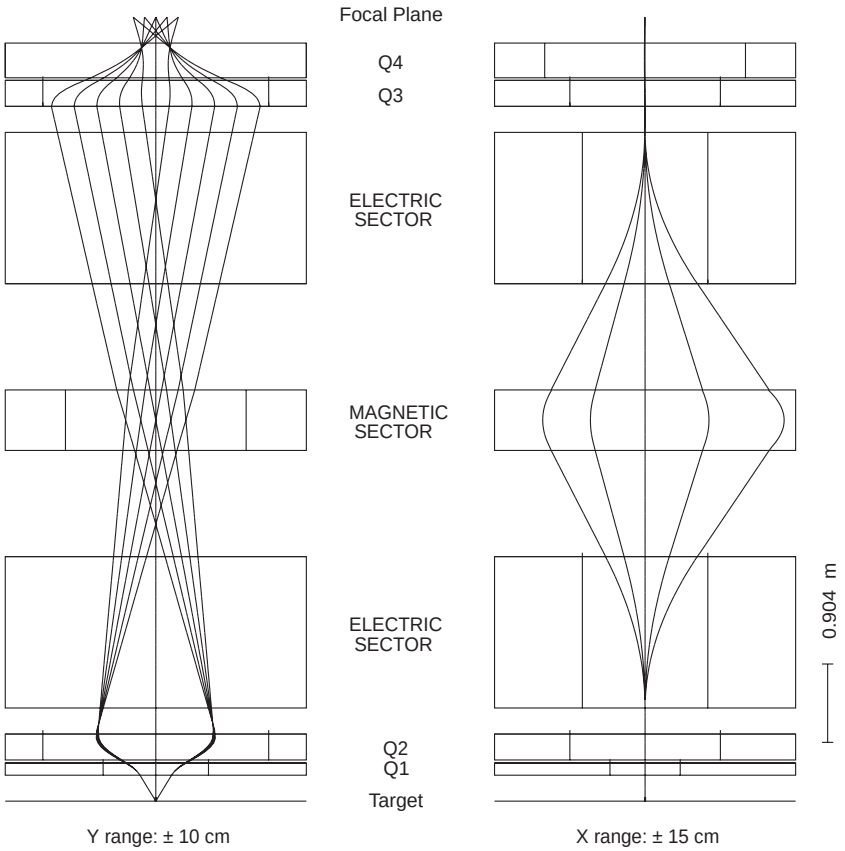

Fig. 3. Calculated energy focus of EMMA, showing rays corresponding to a single mass emitted from the target with vertical angles of -2°, 0°, and 2°, and with energies deviating from the central value by 0, $\pm 7.5\%$, and $\pm 15\%$. Chromatic aberrations in the vertical direction are evident in the vertical extent of the final focus.

emitted between 120° and 180° in the laboratory emerge with laboratory scattering angles of less than 4 mrad, and an energy spread $\Delta E/E < \pm 0.1\%$ for ^{133}Sn excitation energies up to 5 MeV. In the following, we restrict our attention to these recoils.

We assume a $100\,\mu g\,cm^{-2}$ $(CD_2)_n$ reaction target. Using the longitudinal beam emittance of ISAC-II of 2π keV/u ns with 100 ps beam pulses, the 1σ beam energy spread will be $\pm 0.17\%$ at 6 MeV/nucleon. Including the effects of target thickness and reaction kinematics, after emerging from the target the beam will have an energy spread of $\pm 0.17\%$, and the recoils will have an energy spread of $\pm 0.23\%$, where the beam emittance makes the dominant contribution. The central momenta of beam and recoil, which will have the same charge state distribution, differ relatively by only 2.4×10^{-3}, with the beam having a smaller momentum. However, the 2σ upper limit of the beam momentum differs by only 7.7×10^{-4} relative to the central momentum of the recoils, and is larger than the 1σ lower limit of the recoil momentum distribution. Hence there is a substantial overlap in the magnetic rigidities of the beam and recoil, and if one were to attempt to separate them in a magnetic spectrometer, one would expect more than 10^5 beam particles for every good recoil in the overlap region. This situation is illustrated in Fig. 6, which clearly shows why a magnetic spectrometer is ill-suited for this task.

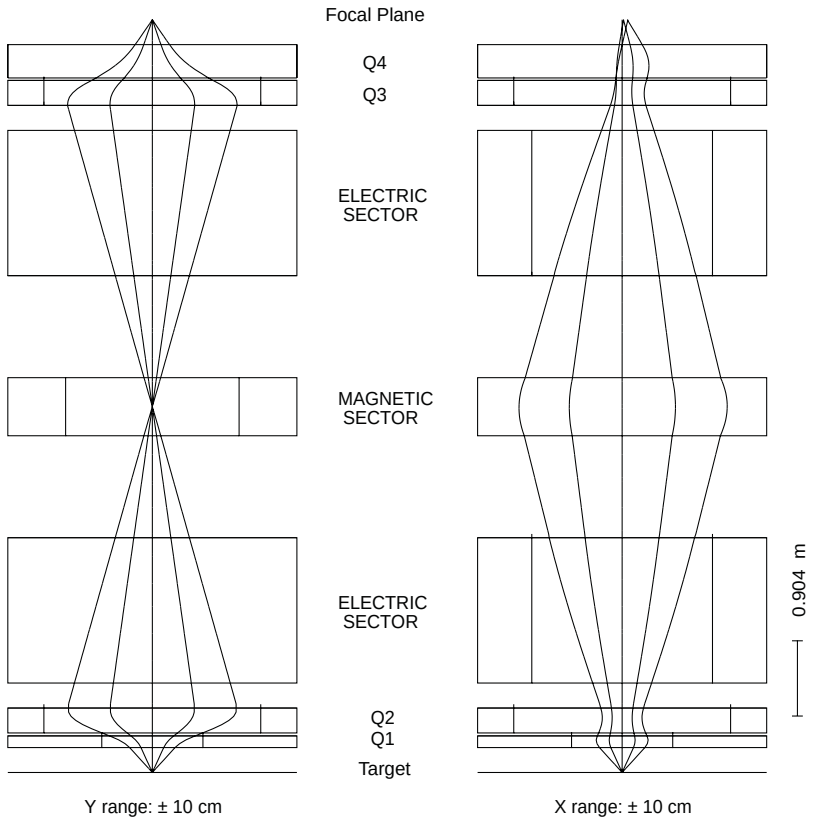

Fig. 4. Calculated spatial focus of EMMA, showing rays corresponding to a single mass emitted from the target with angles of 0, $\pm 1.5^{\circ}$, and $\pm 3^{\circ}$ in the vertical and horizontal directions. The dominant geometric aberration in the dispersive direction, proportional to the square of the horizontal angle, is evident in the horizontal extent of the final focus.

The recoils and beam will emerge from the reaction target with an identical charge state distribution peaked at 41^{+}. The recoils, which have a central energy of 782 MeV, have an electric rigidity of 38 MV, some 50% larger than the maximum for EMMA. Hence we must employ a degrader foil to slow the beam and recoils. We consider here a gold foil of 8.8 μm ($17\,\mathrm{mg\,cm^{-2}}$) thickness located just downstream of the reaction target. The code SRIM 2003 [36] was used to compute energy losses and multiple scattering in the reaction target and degrader foil. Recoil scattering angles after the target are not increased appreciably from the value of 4 mrad given by the reaction kinematics, due to the very thin target. However, the degrader foil substantially broadens the angular distributions of both recoils and beam, with a plane-projected multiple scattering angle distribution characterized by a standard deviation $\sigma = 22$ mrad. While the energy straggling in the degrader is insignificant, resulting in a 2σ energy spread less than 1%, the mean energies of beam and recoils are reduced to 325 and 322 MeV, respectively. This is well below the maximum energy that can be bent for the most probable charge state of 37^{+}, 463 MeV. In this way we use a degrader foil to reduce the electric rigidity of the recoils at the cost of an increased angular divergence. However, the angular acceptance of EMMA is large enough that considerably more than 95% of the recoils in this most probable charge state will reach the focal plane. The focal plane image for a uniform energy spread of ±1% and uniform angular spreads of $\pm 3^{\circ}$ in the vertical

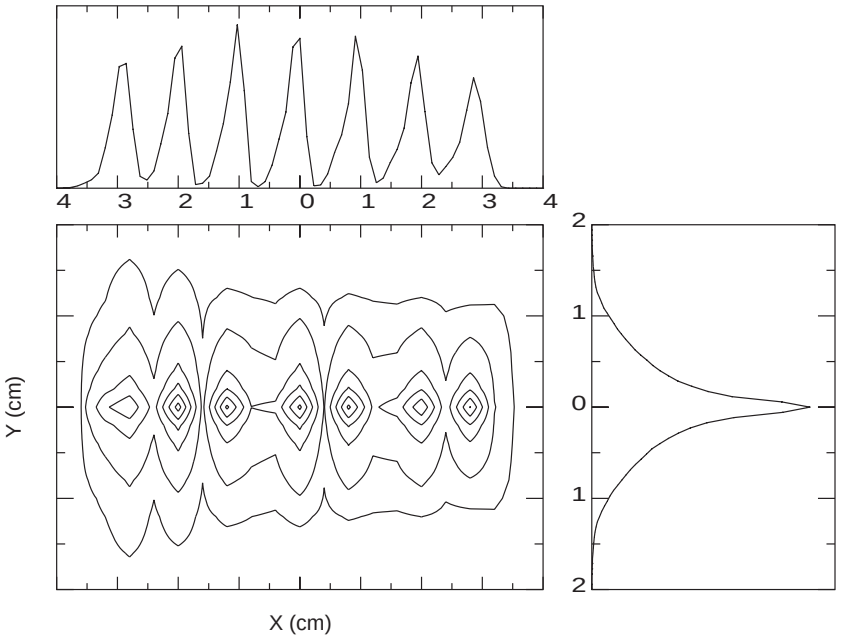

Fig. 5. Calculated M/q spectrum of EMMA centred about mass 100, showing 7 adjacent masses from 97 to 103 emitted from the target with uniform angular spreads of $\pm 3^\circ$ in the horizontal and vertical directions, and a uniform energy distribution of $\pm 10\%$.

Table 2
Calculated properties of EMMA

Horizontal magnification	-2.08
Vertical magnification	1.33
M/q dispersion (variable)	0–20 mm/%
First-order M/q resolving power (1 mm beam spot, 10 mm/% dispersion)	481
Horizontal angular acceptance for central mass and energy	$\pm 3.6^\circ$
Vertical angular acceptance for central mass and energy	$\pm 3.6^\circ$
Solid angle for central M/q and energy	16 msr
M/q acceptance	$\pm 4\%$
Energy acceptance for central mass and angle	$^{+25\%}_{-17\%}$
M/q resolving power for $\pm 3^\circ \times \pm 3^\circ$ (11 msr) and $\Delta E/E = \pm 10\%$	368 FWHM

and horizontal directions was calculated with GIOS and is shown in Fig. 7. This calculation is conservative in that the angular distribution was assumed to be uniform rather than Gaussian. Nevertheless, it shows that the spatial distributions of recoils and beam particles overlap, which is problematic. Note that the mass resolving power for this case, 379 FWHM, is inadequate for the task. This underscores the fact that the separation of recoils and beam in a single-nucleon transfer reaction induced by a heavy beam in inverse kinematics requires high mass resolution. Of course, the actual degree of separation depends on the transfer reaction cross-section. Here we have assumed a single recoil for every 5×10^6 beam particles, which corresponds to a realistic cross-section of 30 mb.

The separation between beam and recoils at the focal plane also depends on the details of the line shape. The long tails of the mass peaks in Fig. 7 are due to the dominant $(x|a^2)$ aberration. By reducing the horizontal scattering angle acceptance to $\pm 2^\circ$ through the use of an aperture in the target chamber, the mass resolution can be substantially improved without an unacceptable sacrifice of yield. Fig. 8 shows the mass spectrum obtained in this case. Restricting the horizontal angular acceptance in this way still allows 82% of the recoils to enter EMMA. The charge states

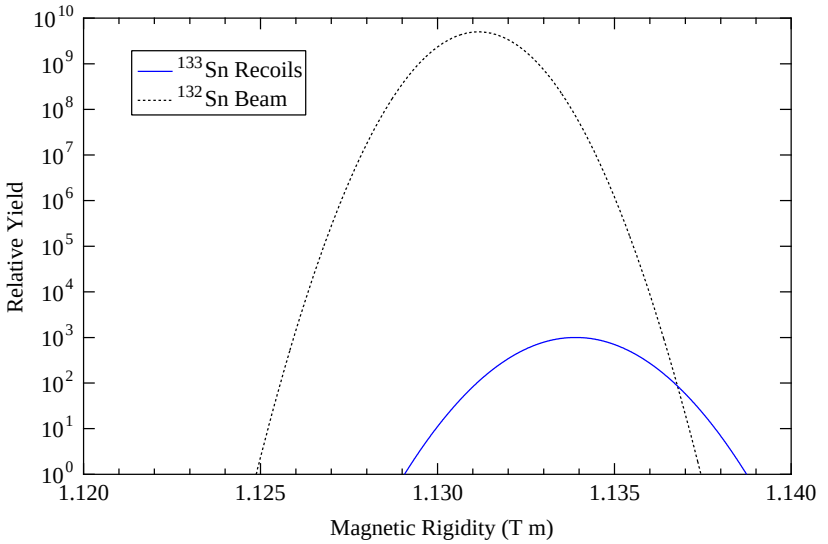

Fig. 6. Magnetic rigidities of beam and recoils from d(^{132}Sn,p)^{133}Sn at 6 MeV/nucleon, calculated for a 100 μg cm^{-2} $(CD_2)_n$ target and a realistic ISAC-II beam energy spread of ±0.17% (1σ). This figure dramatically illustrates why a magnetic spectrometer cannot be used to separate beam and recoils in this reaction.

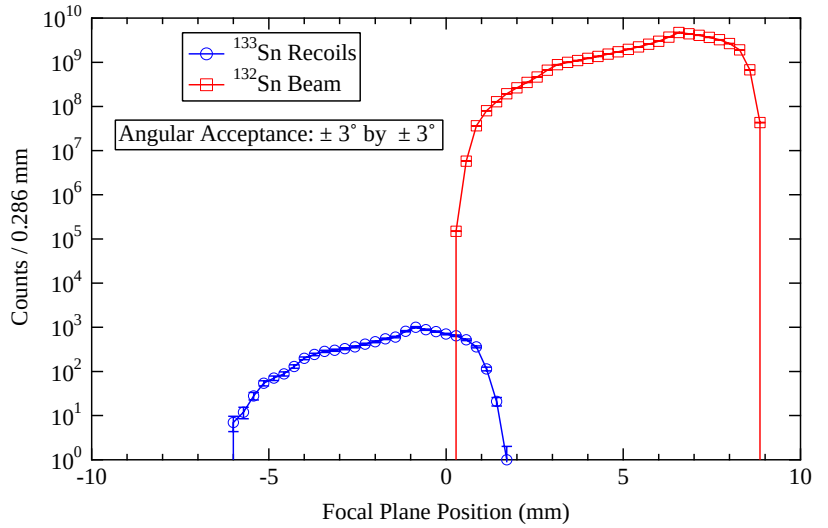

Fig. 7. Simulated mass-dispersive focal plane image from d(^{132}Sn,p)^{133}Sn at 6 MeV/nucleon, showing inadequate spatial separation between beam and recoils. Realistic ISAC-II beam emittances were used. The ions were propagated through a 100 μg cm^{-2} $(CD_2)_n$ target and a 17 mg cm^{-2} gold energy degrader using SRIM 2003, and through EMMA using the ion optics code GIOS.

36^+ and 38^+ will also be transmitted to the focal plane, along with the corresponding charge states of the beam, which will be stopped on slits. The geometric transmission efficiency for these three charge states through EMMA is 99%, so the only substantial losses are due to the M/q acceptance. Since these three charge states comprise an estimated 47% of the total charge state

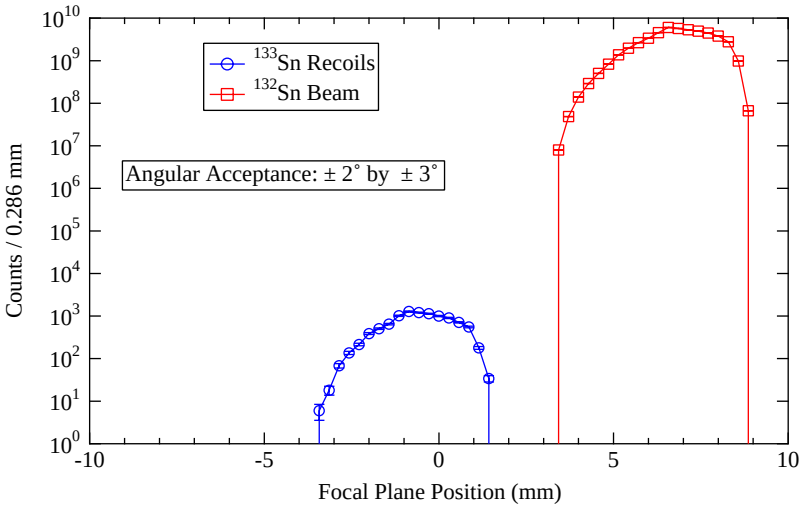

Fig. 8. Same as the previous figure, but with limited horizontal angular acceptance. The mass resolving power of 430 FWHM, obtained by limiting the horizontal scattering angle range, is seen to be sufficient.

distribution, we calculate an overall transmission efficiency of 38% for the interesting recoils. In this way, we see that by employing an energy degrader and placing slits at the mass focus we can achieve excellent beam suppression and transmission efficiency for the recoils of a single-nucleon transfer reaction at mass 132 above the Coulomb barrier.

6. Summary

A preliminary design of EMMA, an electromagnetic mass analyzer for ISAC-II at TRIUMF was presented. EMMA is a recoil mass spectrometer that will be used to separate the recoils of nuclear reactions from the beam, and to disperse them according to mass/charge. ISAC-II will provide intense, low-emittance beams of unstable nuclei with masses up to 150 u and maximum energies of at least 6.5 MeV/nucleon. EMMA will be used in many different types of experiments with radioactive beams, especially in the study of fusion-evaporation reactions and transfer reactions in inverse kinematics. As such, it must be both efficient and selective, possessing large acceptances in angle, mass, and energy without sacrificing the necessary beam suppression and mass resolution. Ion optical calculations and a simulation of a (d,p) reaction in inverse kinematics with a heavy beam above the Coulomb barrier were presented, demonstrating that the design goals have been met.

Acknowledgements

This work was supported by the Natural Sciences and Engineering Research Council of Canada and by the U.S. Department of Energy, Office of Nuclear Physics, under contract No. W-31-109-ENG-38.

References

[1] R.E. Laxdal, et al., in: Proceedings of the 2003 Particle Accelerator Conference, IEEE, 2003, p. 601.
[2] G. Münzenberg, et al., Nucl. Instr. and Meth. 186 (1979) 423.
[3] M. Leino, et al., Nucl. Instr. and Meth. B 99 (1995) 653.
[4] A.M. Stefanini, et al., LNL Annual Report 2003, INFN, 2004, p. 139.
[5] A. Cunsolo, et al., Nucl. Instr. and Meth. A 484 (2002) 56.
[6] H. Savajols, Nucl. Instr. and Meth. B 204 (2003) 146.
[7] T.M. Cormier, P.M. Stwertka, Nucl. Instr. and Meth. 184 (1981) 423.
[8] T.M. Cormier, P.M. Stwertka, Nucl. Instr. and Meth. 212 (1983) 185.

[9] M. Leino, Nucl. Instr. and Meth. B 204 (2003) 129.
[10] C.N. Davids, Nucl. Instr. and Meth. B 204 (2003) 124.
[11] C.E. Svensson, et al., Nucl. Instr. and Meth. B 204 (2003) 660.
[12] T. Davinson, et al., Nucl. Instr. and Meth. A 454 (2000) 350.
[13] G. Münzenberg, Nucl. Instr. and Meth. B 70 (1992) 265.
[14] J.S. Winfield, W.N. Catford, N.A. Orr, Nucl. Instr. and Meth. A 396 (1997) 147.
[15] H. Savajols, Talk at TRIUMF EMMA Workshop, 2003.
[16] P. Spolaore, J.D. Larson, et al., Nucl. Instr. and Meth. A 238 (1985) 381.
[17] C. Signorini, et al., Nucl. Instr. and Meth. A 339 (1994) 531.
[18] P. Spolaore, et al., Nucl. Instr. and Meth. A 359 (1995) 500.
[19] C.N. Davids, J.D. Larson, Nucl. Instr. and Meth. B 40 (1989) 1224.
[20] C.N. Davids, et al., Nucl. Instr. and Meth. B 70 (1992) 358.
[21] B.B. Back, et al., Nucl. Instr. and Meth. A 379 (1996) 206.
[22] T.M. Cormier, et al., Nucl. Instr. and Meth. A 297 (1990) 199.
[23] J.D. Cole, et al., Nucl. Instr. and Meth. B 70 (1992) 343.
[24] C.J. Gross, et al., Nucl. Instr. and Meth. A 450 (2000) 12.
[25] A.K. Sinha, et al., Nucl. Instr. and Meth. A 339 (1994) 543.
[26] H. Ikezoe, et al., Nucl. Instr. and Meth. A 376 (1996) 420.
[27] H. Ikezoe, et al., Nucl. Instr. and Meth. B 126 (1997) 340.
[28] T. Kuzumaki, H. Ikezoe, et al., Nucl. Instr. and Meth. A 437 (1999) 107.
[29] D.A. Hutcheon, et al., Nucl. Instr. and Meth. A 498 (2003) 190.
[30] S. Morinobu, et al., Nucl. Instr. and Meth. B 70 (1992) 331.
[31] A.N. James, et al., Nucl. Instr. and Meth. A 267 (1988) 144.
[32] M. Couder, et al., Nucl. Instr. and Meth. A 506 (2003) 26.
[33] D. Rogalla, et al., Nucl. Instr. and Meth. A 513 (2003) 573.
[34] H. Wollnik, J. Brezina, M. Berz, Nucl. Instr. and Meth. A 258 (1987) 408.
[35] H. Wollnik, Optics of Charged Particles, Academic Press, Inc., New York, 1987.
[36] J.F. Ziegler, Nucl. Instr. and Meth. B 219–220 (2004) 1027.